Thermomechanical processing effects on the martensitic transformation in Fe-based SMAs

E. MIHALACHE[a], F. BORZA[b], N. LUPU[b], N. M. LOHAN[a], B. PRICOP[a], M.-G. SURU[a*], L.-G. BUJOREANU[a]
[a] *Faculty of Materials Science and Engineering, The "Gheorghe Asachi" Technical University of Iaşi, Bd. D. Mangeron 67, 700050 Iaşi, Romania*
[b] *National Institute of Research and Development for Technical Physics, Bd. D. Mangeron 47, 700050, Iaşi, Romania*

Magnetic shape memory alloys (MSMAs) belonging to Fe-Ni-Co-Al system have been recently developed due to their small temperature dependence of superelastic and magnetic properties, which renders great potential for practical applications. Specimens of $Fe_{40.95}Ni_{28}Co_{17}Al_{11.5}Ta_{2.5}B_{0.05}$ (at.%) were obtained under the form of melt spun ribbons. The ductility of the specimens was improved by precipitation-hardening heat treatments, meant to enable the occurrence of nanometric-size γ' particles. The structure of rapidly quenched specimens was analyzed by X-Ray diffraction (XRD) and scanning electron microscopy (SEM). Thermal behaviour was evaluated by differential scanning calorimetry (DSC), from a thermodynamic point of view, aiming to emphasize solid state transitions and by thermomagnetic measurements, from a magnetic point of view, aiming to reveal magnetization dependence on both applied magnetic field and temperature-. Finally, the superelastic behaviour was investigated by micro-indentation. The experimental data allowed analyzing the influence of various factors, such as alloy structure (bulk and rapidly quenched), thermomechanical processing (hot rolling, heat treatment) and precipitation hardening temperature on the structure and properties of Fe-Ni-Co-Al MSMAs.

(Received April 9, 2015; accepted September 9, 2015)

Keywords: Magnetic shape memory alloys, Structure, Thermomechanical treatment, Magnetism, Superelasticity

1. Introduction

Metallic materials that show the ability to return to their initial shape when subjected to a heating process are called shape memory alloys (SMAs). Shape memory effect (SME) was first reported in 1938 in a Cu-Zn alloy and was observed in 1951 in a bent bar of AuCd. Due to their properties, SMAs as Ni-Ti and Cu-Zn-Al, experience large reversible strains either by SME or by superelasticity (SE) [1].

Presently, most of SMAs practical applications are encountered at Ni-Ti-base alloys because they show excellent superelastic strains and good ductility. Polycrystalline alloys such as Fe-Mn-Si, Fe-Ni-C and Fe-Ni-Co-Ti, have been developed as "ferrous SMAs" because their workability is better, their cost is lower and are beginning to be more commercially attractive than Ni-Ti-based SMAs. The disadvantage is that, at room temperature, the superelasticity can hardly be showed in this "ferrous SMAs", because their martensitic transformations, γ [face centre cubic (fcc)]→ε [hexagonal close packed (hcp)] or γ→α′ [body centre cubic (bcc)] or [body centre tetragonal (bct)] are basically nonthermoelastic [2]. Though Fe-Pd and Fe-Pt alloys exhibit a thermoelastic fcc face-centred tetragonal→(fct) transformation, no superelasticity at room temperature was reported long time after the discovery of Fe-Ni-Co-Ti alloy in 1984 [3].

In 2010, ferrous polycrystalline Fe-28Ni-17Co-11.5Al-2.5Ta-0.05B (at.%) SMA was reported which, in aged state with {035}<100> texture at room temperature, experienced a superelastic strain over 13%, associated with thermoelastic γ (fcc)→α′(bct) transformation [4]. This ferrous SMA has great potential as multifunctional material for a wide variety of engineering applications [5].

However, no reports can be found on the structure and properties of this promising alloy, when processed by melt spinning, which has the potential to drastically reduce grain size in such a way as to enhance mechanical properties [6].

The purpose of the present paper has been to analyze both superelastic and magnetic properties, in melt spun Fe-28Ni-17Co-11,5Al-2.5Ta-0.05B (at.%) ribbons and to discuss heat treatment and melt spinning parameters effects on these properties.

2. Materials and methods

$Fe_{40.95}Ni_{28}Co_{17}Al_{11.5}Ta_{2.5}B_{0.05}$ ribbons with two thickness/ width ratios, 20/ 58 and 43/ 70 (10^{-6} m/ 10^{-6} m), were been prepared by melt spinning [7]. The former were designated as narrow ribbons (NR) and the latter as wide ribbons (WR). Ta was used to stabilize γ' phase and to increase its volume fraction, causing hardness increase and inducing thermoelastic character to martensite transformation. Melt spun ribbons were subjected to heat treatment for 3.6 ks at 473 K.

X-Ray diffraction (XRD) measurements were done using a D8 Advance - Bruker AxS GmbH diffractometer with Cu-Kα radiation to determine phase structure, considering the lattice parameters for γ (fcc) as a = 0.3604

nm and for α′ (bct) martensite as a = 0.2771 nm and c = 0.3069 nm [4].

Scanning electron microscopy (SEM) and electron backscatter diffraction (EBSD) observations were performed using a JEOL JSM 6390 microscope.

Micro-indentation tests were performed with a UMT-CETR universal tester at a maximum load of 13.5 N. More details on specimens' preparation and test parameters were previously detailed [8].

Thermo-magnetic and magnetic measurements have been carried out on a VSM Lakeshore magnetometer, in a maximum applied field of 600 kA/m, to assess the structural and magnetic differences between melt spun and heat treated samples.

3. Results and discussion

The representative XRD patterns for the two types of ribbons, both in melt spun and heat treated states, are summarized in Fig.1. Figure 1(a) corresponds to narrow ribbons (NR) and 1(b) to wide ribbons (WR).

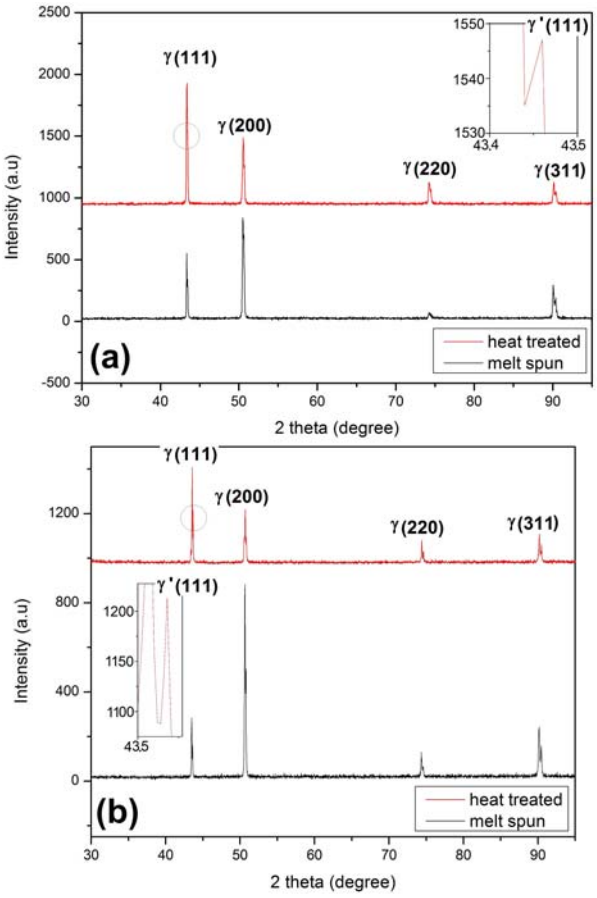

Fig. 1. Representative XRD patterns for the two types of $Fe_{40.95}Ni_{28}Co_{17}Al_{11.5}Ta_{2.5}B_{0.05}$ ribbons in melt spun and heat treated states: (a) narrow ribbons (NR); (b) wide ribbons (WR).

On both patterns four major diffraction maxima are noticeable which were ascribed to γ(111), γ(200), γ(220) and γ(311). In both cases, the heat treatment caused a change in ribbon texture in such a way that γ-phase became reoriented in such a way that the plane parallel to ribbon surface is now (200) instead of (111), which is the main close packed plane for fcc structures.

A detail of this particular diffraction maximum reveals a smaller maximum which can be associated with the formation of γ'(111) precipitates [9]. Considering that γ' precipitates do not undergo martensitic transformation, they favour the accumulation of the elastic energy in martensite crystals [10] thus changing the kinetics of transformation from a nonthermoelastic, with large temperature hysteresis (approx. 400 K), to a thermoelastic one, with smaller hysteresis (30–100 K) in the heterophase state [11]. The two magnified details of γ'(111) maxima obviously reveal that in heat treated wide ribbons (WR), Fig.1(b), the formation of a larger precipitate amount was enhanced. A simple calculation of phase relative amounts gives approx. 10 % γ'-phase in WR. On the other hand, in heat treated narrow ribbons (NR) the amount of γ'-phase can be estimated to about 1 %. This could be a consequence of the smaller cross-section of NR (20 × 58 10^{-6} m) as compared to WR (43 × 70 10^{-6} m).

After melt spinning, the amorphisation degree would be higher in thinner NR in such a way that the heat treatment applied for 3.6 ks at 473 K was not sufficient to enable the precipitation of γ'-phase [12]. For this reason further discussion will be focused on data obtained on heat treated WR.

SEM observations revealed the formation of small grains (of the order of micrometers) in melt spun samples. After heat treatment, full austenitization occurred and a typical γ-phase microstructure for Fe-Ni-Co base alloys was observed [13]. Average grain size slightly increased, up to 10 micrometers.

Figure 2, obtained by electron back scattering (ESB), summarizes the main morphological features of heat treated WR. In the general SEM micrograph, shown in Fig.2(a), the dispersion of small white precipitates is noticeable both within austenitic grains and along grain boundaries. Even at larger magnifications, as in Fig.2(b), there is no trace of γ'-phase precipitates due to their very small size [14]. Moreover neither martensite could be detected, in good agreement with XRD patterns.

The average size of white precipitates can be estimated to 90 nm. By EDX it was determined that they are Ta-rich particles.

The total absence of martensite plates, which are indispensable for a Fe-Ni-Co alloy to exhibit shape memory effect (SME) [15] sustains the assumption that martensite cannot be stabilized at room temperature and for this reason WR specimens meet the conditions to be superelastic since α' martensite would be stress-induced from austenite during loading and would revert to austenite during unloading.

This lack of stability of stress-induced martensite, in Fe-based SMAs, is the first prerequisite for the obtainment of a superelastic response [16].

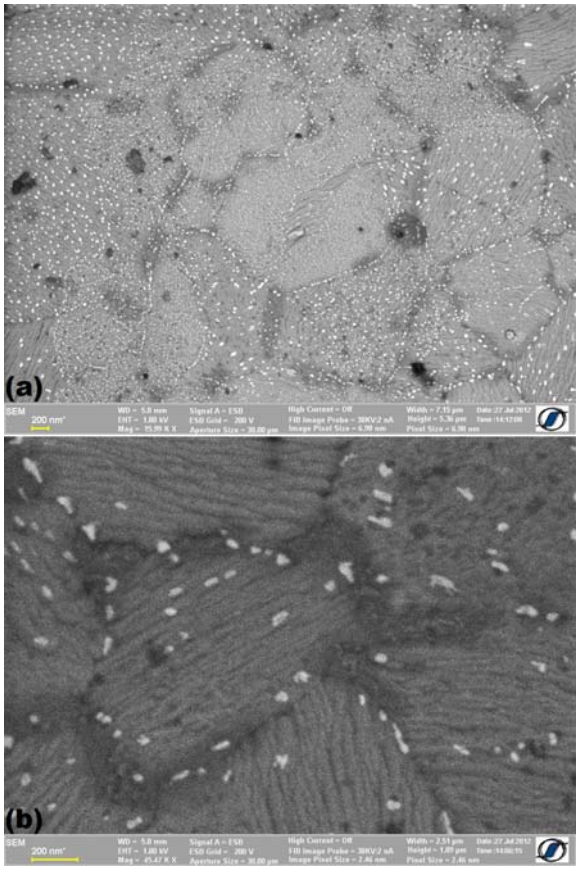

Fig. 2. Typical SEM micrographs of heat treated $Fe_{40.95}Ni_{28}Co_{17}Al_{11.5}Ta_{2.5}B_{0.05}$ WR: (a) general aspect, revealing the dispersion of white Ta-rich precipitates; (b) detail of a single austenite grain with Ta-rich precipitates.

In order to verify the reversible stress-induced formation of α′ martensite, which is the mechanism of superelasticity (SE), micro-indentation tests were performed on WR specimens. A representative curve is shown in Fig.3, with a SE response, characterized by two distinctive stress-variation segments on both loading and unloading portions. The second unloading stress segment, obtained at very low loads, is almost a plateau and represents the main feature of a superelastic response.

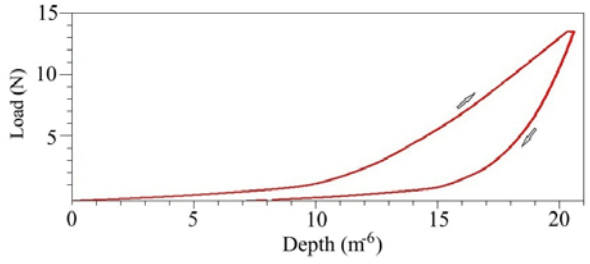

Fig. 3. Typical micro-indentation curve of heat treated $Fe_{40.95}Ni_{28}Co_{17}Al_{11.5}Ta_{2.5}B_{0.05}$ WR revealing a superelastic response of 63 %.

It is noticeable that austenite does not undergo any elastic deformation, during micro-indentation, since the transformation plateau (which is typically horizontal) starts in the same time with the test, directly from zero load.

α′ stress-induced formation can be considered as perfected after an indentation depth of 10 μm. Further loading caused elastic deformation of α′ stress-induced martensite up to a total depth of 20.5 μm. During unloading, α′ martensite was relaxed elastically for about 5 μm and then reverted to austenite, with reverse transformation plateau of approx. 8 μm. At the end of the test a residual depth of approx. 7.5 μm was obtained. Considering recoverable depth as 20.5-7.5=13 μm, it follows that micro-indentation depth recovery degree through superelasticity was SE%=13/20.5×100 ≈ 63 %, which is fairly comparable with similar results reported on Fe-Ni based SMAs [17]. These results confirm that the role of γ'-phase, as γ-phase matrix strengthening precipitates, has been successfully fulfilled in the case of heat treated melt spun wide ribbons.

Magnetic measurements have been performed in order to assess the changes induced by low temperature thermal treatment in the magnetic behaviour of samples, Fig.4(a) and (b).

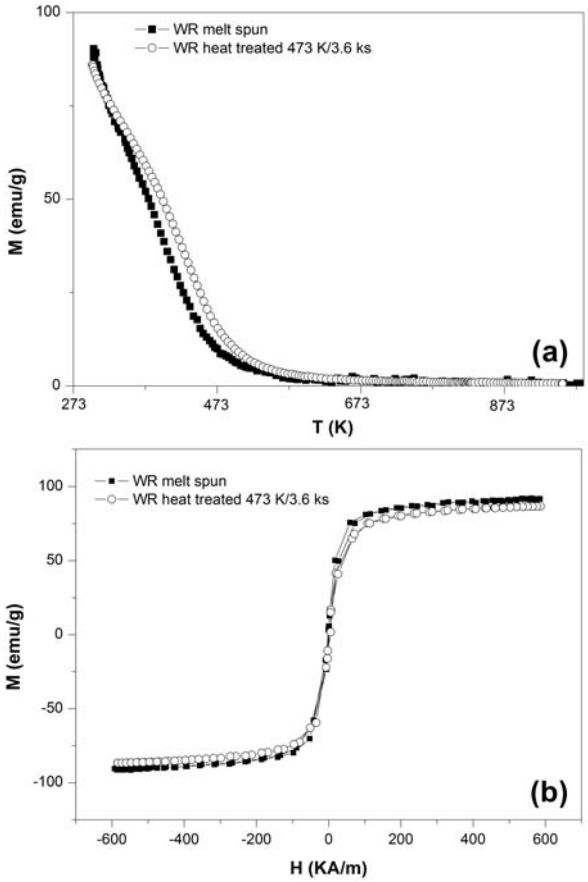

Fig. 4. Thermomagnetization curves (a) and hysterezis loops (b) of melt spun and heat treated $Fe_{40.95}Ni_{28}Co_{17}Al_{11.5}Ta_{2.5}B_{0.05}$ WR.

Fig.4 (a) shows the magnetization versus temperature (M-T thermo-magnetic curves) measured in a maximum applied magnetic field of 600 kA/m of the WR sample in melt spun state and after the heat treatment at 473 K for 3.6 ks, respectively. For both melt spun and heat treated specimens the magnetization decreases abruptly with the increase in the temperature, from room temperature up to the Curie temperature, T_c, because of phase transitions [18] and remains constant up to 973 K. The Curie temperatures of melt spun and heat treated specimens are 478 K and 513 K, respectively. The difference in T_c between the two specimens can be attributed to the formation of the γ'-phase [19] after heat treatment.

The change in the hysteresis loops, Fig.4 (b), confirms the above mentioned behaviour. The coercive field increases from 1.6 kA/ m, to 2.6 kA/m after the heat treatment while the saturation magnetization slightly decreases, due to the formation of crystalline grains of γ'-phase. The inclination of the hysteresis loop increases for the heat treated specimens with respect to the Y-axis. This behaviour can be ascribed to the combined effect of the formation of the new γ'-phase and to the relaxation of internal stresses induced by the rapid quenching process [20].

4. Summary and conclusions

In melt spun $Fe_{40.95}Ni_{28}Co_{17}Al_{11.5}Ta_{2.5}B_{0.05}$ ribbons, with a cross-section of 20 × 58 10^{-6} m, which were heat treated for 3.6 ks at 473 K, a superelastic response was obtained by micro-indentation tests which was associated with the reversible stress-induced martensitic transformation from γ-phase austenite matrix which was reinforced by the precipitation of approx. 10 % γ'-phase with an average size of 85 10^{-6} m. The superelastic response, characterized by a shape recovery degree of 63 % is comparable to that reported by Tanaka et al. in bulk textured Fe-Ni-Co-Al-Ta-B SMAs being much more prominent as compared to the pseudoelastic spring-back reported at bulk specimens of Fe-Mn-Si-Cr-Ni SMA, obtained by classical metallurgy [21].

A slight change in the magnetic properties has been induced by the formation of γ'-phase and due to the thermal relieve of internal stresses. The Curie temperature increased with about 35 K, the coercive field increased, from 1.6 kA/m to 2.6 kA/m, indicating the strengthening of the magnetic hard phase.

Work is in progress to find the temperature-time conditions for the achievement of the optimum mechanical and magnetic properties which will make this rapidly quenched material a potential competitor for the conventional superelastic alloy.

Acknowledgements

This research work was supported by the project PN-II-ID-PCE-2012-4-0033, contract 13/ 2013.

References

[1] D. E. Hodgson, H. W. Ming, R. J. Biermann, Shape memory alloys, ASM Handbook, **2**, 897 (1990)
[2] D. Dunne, Phase transformations in steels, **2**, 83 (2012)
[3] T. Maki, Shape Memory Materials, 117 (1998)
[4] Y. Tanaka, Y. Himuro, R. Kainuma, Y. Sutou, T. Omori, K. Ishida, Science, **327**, 1488 (2010)
[5] J. Ma, B. Kockar, A. Evirgen, I. Karaman, Z.P. Luo, Y.I. Chumlyakov, Acta Mater, **60**, 2186 (2012)
[6] M. Izadinia, K. Dehghani, T Nonferr Metal Soc, **21** (9), 2037 (2011)
[7] F. Borza, A. L. Paraschiv, L. G. Bujoreanu, N. Lupu, ICPAM-9, (2012)
[8] M.-G. Suru, I. Dan, N. M. Lohan, A. L. Paraschiv, B. Pricop, I. P. Spiridon, C. Baciu, L.-G. Bujoreanu, Materialwiss Werkst, **45** (1), 44 (2014)
[9] Y. Geng, M. Jin, W. Ren, W. Zhang, X. Jin, J Alloy Compd, doi:10.1016/j.jallcom.2012.03.033, (2012)
[10] Y. I. Chumlyakov, I. V. Kireeva, E. Y. Panchenko, E. G. Zakharova, V. A. Kirillov, S. P. Efimenko, H. Sehitoglu, Dokl Phys, **49** (1), 47 (2004)
[11] Y. I. Chumlyakov, I. V. Kireeva, E. Y. Panchenko, V. B. Aksenov, V. A. Kirillov, A. V. Ovsyannikov, E. G. Zakharova, H. Sehitogly, Russ Phys J, **46**(8), 811 (2003)
[12] T. Todaka, S. Teshima, M, Enokizono, J Mater Process Tech, **181**, 217 (2007)
[13] A. N. Titenko, L. D. Demchenko, J Mater Eng Perform, **21**(12), 2525 (2012)
[14] M.-G. Suru, L.-G. Bujoreanu, Materialwiss Werkst, **43**(11), 973 (2012)
[15] R. Hayashi, S.J. Murray, M. Marioni, S.M. Allen, R.C. O'Handley, Sensors Actuat A, **81**, 219 (2000)
[16] L. G. Bujoreanu, V. Dia, S. Stanciu, M. Susan, C. Baciu, Eur. Phys J. Special Topics, **158**, 15 (2008)
[17] Y. Liao, I. Baker, Mat Sci Eng A, **528**(12), 3998 (2011)
[18] A. Amengual, V. Torra, Thermochimica Acta, **198** (2), 381 (1992)
[19] H. Li, D. Dunne, N. Kennon, Mat Sci Eng A, **273-275**, 517 (1999)
[20] P. Duwez, J. Vac. Sci. Technol. B, **1**, 218 (1983)
[21] L. G. Bujoreanu, S. Stanciu, B. Özkal, R. I. Comăneci, M. Meyer, ESOMAT 2009, 05003 (2009)

*Corresponding author: marius_suru2005@yahoo.com